

Research Article

Multiobjective Genetic Algorithm and Convolutional Neural Network Based COVID-19 Identification in Chest X-Ray Images

Prashant Kumar Shukla,¹ Jasmininder Kaur Sandhu², Anamika Ahirwar³,
Deepika Ghai,⁴ Priti Maheshwary,⁵ and Piyush Kumar Shukla⁶

¹Department of Computer Science and Engineering, University Institute of Technology,
Rajiv Gandhi Proudlyogiki Vishwavidyalaya (Technological University of Madhya Pradesh), Bhopal (MP), India

²Chitkara University Institute of Engineering and Technology, Chitkara University, Rajpura, Punjab, India

³Department of Science and Technology, Jayoti Vidyapeeth Women's University, Jaipur, Rajasthan, India

⁴Lovely Professional University, Jalandhar, India

⁵Department of Computer Science and Engineering, Rabindranath Tagore University, Bhopal, India

⁶Department of Computer Science and Engineering, University Institute of Technology,
Rajiv Gandhi Proudlyogiki Vishwavidyalaya (Technological University of Madhya Pradesh), Bhopal (MP), India

Correspondence should be addressed to Piyush Kumar Shukla; pphdws@gmail.com

Received 28 May 2020; Accepted 1 October 2020; Published 25 February 2021

Academic Editor: Manjit Kaur

Copyright © 2021 Prashant Kumar Shukla et al. This is an open access article distributed under the Creative Commons Attribution License, which permits unrestricted use, distribution, and reproduction in any medium, provided the original work is properly cited.

COVID-19 is a new disease, caused by the novel coronavirus SARS-CoV-2, that was firstly delineated in humans in 2019. Coronaviruses cause a range of illness in patients varying from common cold to advanced respiratory syndromes such as Severe Acute Respiratory Syndrome (SARS-CoV) and Middle East Respiratory Syndrome (MERS-CoV). The SARS-CoV-2 outbreak has resulted in a global pandemic, and its transmission is increasing at a rapid rate. Diagnostic testing and approaches provide a valuable tool for doctors and support them with the screening process. Automatic COVID-19 identification in chest X-ray images can be useful to test for COVID-19 infection at a good speed. Therefore, in this paper, a framework is designed by using Convolutional Neural Networks (CNN) to diagnose COVID-19 patients using chest X-ray images. A pretrained GoogLeNet is utilized for implementing the transfer learning (i.e., by replacing some sets of final network CNN layers). 20-fold cross-validation is considered to overcome the overfitting quandary. Finally, the multiobjective genetic algorithm is considered to tune the hyperparameters of the proposed COVID-19 identification in chest X-ray images. Extensive experiments show that the proposed COVID-19 identification model obtains remarkably better results and may be utilized for real-time testing of patients.

1. Introduction

The initial occurrence of COVID-19 disease was found in Wuhan, China, during December 2019. Ever since, it is increasing at a rapid rate in the entire world. The testing of COVID-19 is time-consuming, and also, the results obtained from rapid COVID-19 testing kits are not reliable. Therefore, radiologists and doctors have started using supervised learning techniques to test COVID-19 disease. The prime objective is to identify COVID-19 patients as infected or not, at a rapid rate [1].

The deep learning techniques may be utilized for COVID-19 patient identification [2]. Figure 1 shows the

different chest X-ray images. It is found that there exists a significant change in the chest X-ray image of COVID-19-infected patients as compared to other images.

Machine learning and deep learning techniques are extensively employed to implement computer-aided identification [1, 3]. It has been observed that these techniques can save significant time of clinical persons and doctors for the examination of medical images such as X-ray and Computed Tomography scan (CT scan) [3, 4]. However, these learning techniques require a significant amount of medical images for training. Also, efficient feature extraction and selection techniques are desirable to achieve significant results [5, 6]. Recently, metaheuristic techniques are also

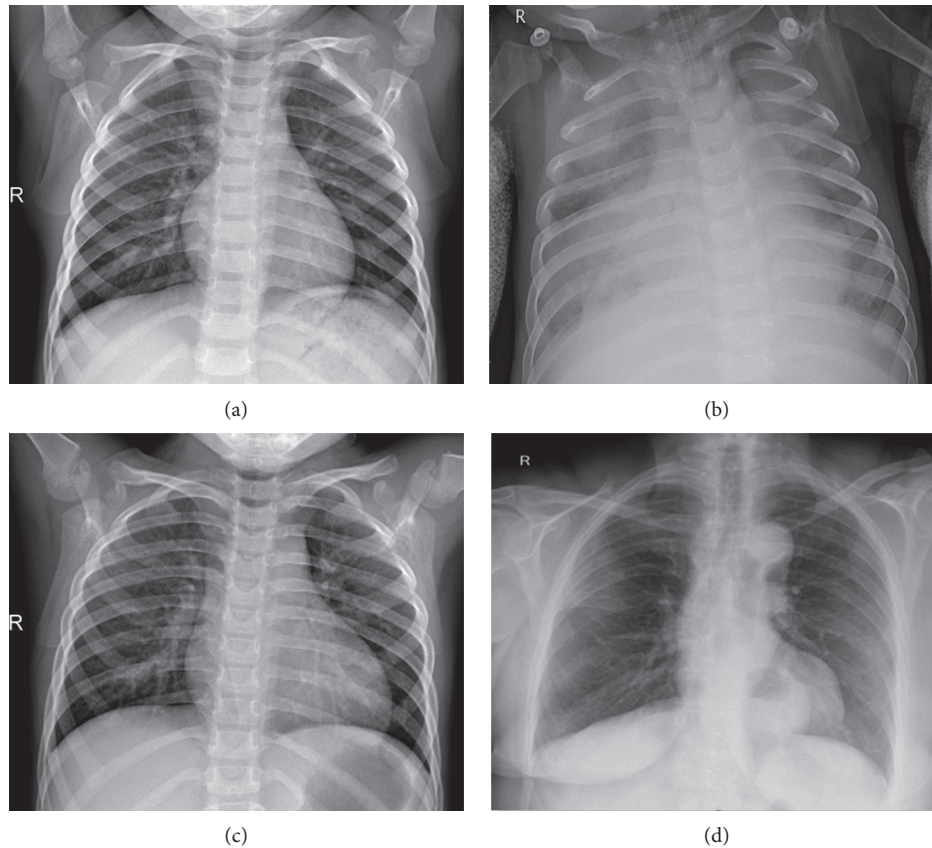


FIGURE 1: Chest X-ray images: (a) healthy, (b) bacterial pneumonia, (c) viral pneumonia (not COVID-19), and (d) COVID-19 infected.

used to tune the hyperparameters of these machine learning models [2, 7].

In this paper, a COVID-19 identification model from chest X-ray images is proposed. The main contributions of this work are as follows:

- (1) The Convolutional Neural Network (CNN) is used to predict COVID-19 disease by using their respective chest X-ray images
- (2) A pretrained GoogLeNet is used for implementing the transfer learning (i.e., by replacing some sets of final network CNN layers)
- (3) 20-fold validation is considered to overcome the overfitting issue
- (4) Finally, the multiobjective genetic algorithm is considered for tuning the hyperparameters of the proposed COVID-19 identification model
- (5) Extensive experiments show that the proposed COVID-19 identification model achieves remarkably good results and may be utilized for real-time testing of patients

The rest of this paper is classified into the following sections. Section 2 presents the related work. The proposed COVID-19 identification model is illustrated in Section 3. Performance analysis is manifested in Section 4. Conclusions are outlined in Section 5.

2. Related Work

This section highlights various techniques that are used to diagnose COVID-19-infected patients from chest X-ray images.

Tang et al. [8] employed GoogLeNet to extract the characteristics of the images. Multistage feature fusion is contemplated to recognize the scene from output characteristics. Gao et al. [9] classified breast cancer by utilizing shallow deep CNN. Deepak and Ameer [10] presented an identification technique using GoogLeNet and deep transfer learning for brain MRI images. Cinar and Yildirim [11] proposed a technique to diagnose the brain tumor using ResNet-50. In this model, the last five layers are removed and eight new layers are appended. Nayak et al. [12] implemented an identification technique through CNN with five layers. This technique comprised four convolutional layers and one fully connected layer.

Liu et al. [13] implemented a ResNet model with multiscale spatiotemporal characteristics. Hao et al. [14] proposed optimized CNN based on target region selection for image recognition. Taheri and Toygar [15] proposed directed acyclic graph-based CNN for identification. It is based on the combination of VGG-16 and GoogLeNet. Ciocca et al. [16] applied CNN to diagnose the images and considered a residual network with 50 layers to extract the characteristics. Liu et al. [17] proposed an identification technique using

optimization of ResNet-50 for remote sensing images. Han and Shi [18] presented a multilead residual neural network to extract the characteristics of ECG records. Talo et al. [19] considered the pretrained models VGG-16, AlexNet, ResNet-18, ResNet-34, and ResNet-50 to automatically diagnose MRI images. They found that ResNet-50 has better accuracy as compared to the other pretrained models.

Das et al. [20] designed a novel extreme version of Inception (Xception) based COVID-19 identification model. Liu et al. [21] suggested an identification model based on ResNet and transfer learning model. In this, a new data augmentation technique is considered with the help of a filter for small datasets. Togacar et al. [22] considered a deep learning model to detect COVID-19 using the X-ray images. The fuzzy color technique is considered to restructure the data classes. MobileNetV2 and SqueezeNet are applied to build the dataset. Social mimic optimization is considered to obtain the feature sets. Further, Support Vector Machine (SVM) is used to diagnose efficient characteristics. Pannu et al. [7, 23] implemented swarm intelligence-based Adaptive Neuro-Fuzzy Inference System (ANFIS) to diagnose COVID-19-infected people.

It has been observed that supervised learning algorithms may be used to test COVID-19 disease from chest X-ray images. Also, the use of pretrained feature extraction models can improve the identification rate [24–27]. The hyperparameter tuning of these models can achieve significant results. The k -fold validation [25] is used to overcome the overfitting problem.

3. Proposed Deep COVID-19 Classification Model

This work used CNN and GoogLeNet for the identification of COVID-19 disease. In addition, a multiobjective genetic algorithm is considered to tune the hyperparameters of the proposed COVID-19 identification model. The step-by-step flow of the designed COVID-19 identification model is discussed in Algorithm 1.

3.1. Transfer Learning Using a Pretrained GoogLeNet. In this work, a GoogLeNet is considered to extract significant characteristics of chest X-ray images. It is a pretrained model, and is used as a transferred source. The characteristics extracted from this layer are considered as transfer learning to build the CNN-based COVID-19 identification model.

3.2. Convolutional Neural Network. CNN is widely used for identification problems [28]. Figure 2 shows the standard architecture of the CNN model. The subsequent sections discuss various layers of CNN.

3.2.1. Convolutional Layer. This layer is considered to build the input characteristics. Various convolution filters are considered to compute the patterns (Figure 3). Each neuron

of the convolutional layer is connected with its sibling neurons to process the feature maps [29, 30].

Every time a convolutional operator provides a new feature map, the feature value y_{ij} in the k^{th} feature map is evaluated as follows:

$$y_{ij,k} = \sum (\mathbf{w}_k \odot \mathbf{x}_{ij}) + b_k, \quad (1)$$

where \mathbf{w}_k and b_k represent the average and bias values of k^{th} mask, \mathbf{x}_{ij} represents the input mask centered at (i, j) , and \odot is the Hadamard product of two matrices.

Weights are shared between sibling nodes to minimize the complexity of the model.

3.2.2. Nonlinear Layer. The nonlinear layer uses an activation function and is implemented on the entire set of feature maps. It can deal with the nonlinear dependencies of the feature maps. In this paper, the ReLu activation function is considered.

3.2.3. Pooling Layer. This layer does not come up with any kind of weights. It endeavors to gain shift invariance by minimizing the feature maps and considering activation properties from the local range of CNN. Average and maximum operators are generally considered in the pooling layer. It uses $k \times k$ mask and produces a unique value. In case of a $N \times N$ layer, the output will be a $N/k \times N/k$ layer.

3.2.4. Fully Connected Layer. This layer considers high-level reasoning. There are connections in every input-output pair. After this layer, other nonlinear functions are used.

3.2.5. Loss Layer. Finally, a loss layer is considered to obtain the trained COVID-19 identification model. For COVID-19 identification, a softmax operator is utilized. Assume that θ defines attributes of CNN such as bias and kernel operators. When obtaining N required sets, $\mathbf{y}^{(i)}$ is the target class considering i^{th} input and $\mathbf{o}^{(i)}$ defines the output of CNN; then, the loss of CNN is computed as follows:

$$\mathcal{L} = \frac{1}{N} \sum_{n=1}^N \ell(\theta; \mathbf{y}^{(n)}, \mathbf{o}^{(n)}). \quad (2)$$

3.3. Multiobjective Fitness Function. The proposed COVID-19 identification model suffers from the hyperparameter tuning problem; therefore, in this paper, a multiobjective genetic algorithm is considered. The performance metrics accuracy (A_c) and F -measure (F_m) are considered to design a multiobjective fitness ($f(t)$) function as

$$f(t) = \begin{cases} \text{maximize } (A_c), \\ \text{maximize } (F_m), \end{cases} \quad (3)$$

where A_c can be evaluated as follows:

$$A_c = \frac{\text{TP} + \text{TN}}{\text{TP} + \text{TN} + \text{FP} + \text{FN}}, \quad (4)$$

- (1) Input: chest X-ray images as a labeled dataset
- (2) Initially, GoogLeNet is utilized to evaluate the significant characteristics of COVID-19 dataset images
- (3) Further, transfer learning is considered to build a CNN-based COVID-19 identification model
- (4) Multiobjective genetic algorithm is utilized to tune the designed model
- (5) Implement k -fold validation to overcome overfitting
- (6) Return tThe constructed COVID-19 identification model for chest X-ray images

ALGORITHM 1: Proposed CNN-based COVID-19 identification model.

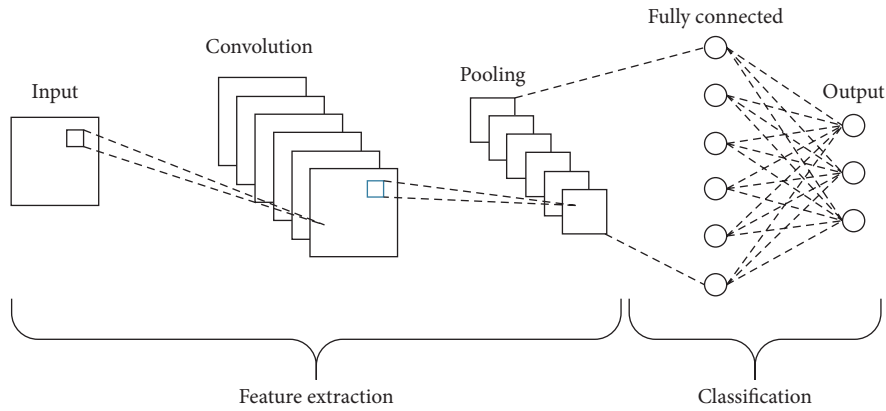


FIGURE 2: Architecture of convolutional neural networks.

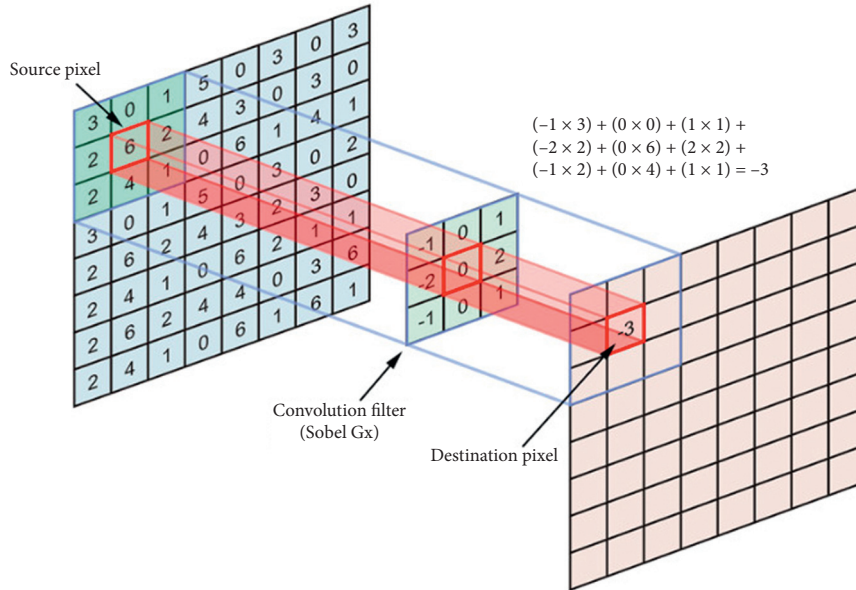


FIGURE 3: Convolutional layer process.

where TP, FP, TN, and FN are the true-positive, false-positive, true-negative, and false-negative values, respectively.

F_m can be evaluated as follows:

$$F_1 = 2 \cdot \frac{p_r \times r_c}{p_r + r_c}, \quad (5)$$

where p_r and r_c represent precision and recall values, respectively. p_r and r_c can be evaluated as follows:

$$p_r = \frac{TP}{TP + FP}, \quad (6)$$

$$r_c = \frac{TP}{TP + FN}. \quad (7)$$

3.4. Multiobjective Genetic Algorithm. The genetic algorithm for Pareto optimization is discussed in Algorithms 2 and 3.

output: $P_f = \{\max. A_c, \max. F_m\}$ /* P_f represents the Pareto front. */

input: COVID-19 training dataset, CNN, random population

begin

- (1) Set random solution as hyperparameters of CNN;
- (2) Apply CNN on COVID-19 training dataset;
- (3) Validate CNN on the same fraction of COVID-19 training dataset;
- (4) Evaluate confusion matrix based on the actual and predicted values;
- (5) $\max. A_c = A_c$ (Confusion matrix);
- (6) $\max. F_m = F_m$ (Confusion matrix);
- (7) **return**{ $\max. A_c, \max. F_m$ }

end

Note. P_f represents the Pareto front.

ALGORITHM 2: Multiobjective optimization.

output: optimized population

input: {Fitness function, demand, crossover_ratio}

begin

- (1) Generate the random I_p ; /* I_p represents the initial population */;
 - (2) Calculate the fitness of I_p ;
 - (3) Sort I_p ;
 - (4) /* Selection */
 - (5) set $F_p = I_p$; /* F_p denotes final population */
 - (6) **while** $c_e \neq 0$ or $l_G == \text{true}$ **do**
 - (7) /* c_e and l_G represent children elimination and last generation */
 - (8) Generate random c ; /* c denotes children */
 - (9) set $c_e = 0$;
 - (10) **for each** c **do**
 - (11) Compute the fitness of c ;
 - (12) **if** $f_c \leq f_{F_p[1]}$ **then**
 - (13) remove c ;
 - (14) set $c_e += 1$;
 - (15) **else**
 - (16) set $F_p = c$;
 - (17) **end**
 - (18) **end**
 - (19) /* Mutation */
 - (20) **for crossover** **do**
 - (21) select c_1 and c_2 randomly; /* c_1, c_2 , and c_3 are children */
 - (22) $c_3 = c_1 \oplus c_2$;
 - (23) Evaluate the fitness of c_3 ;
 - (24) **if** $f_{c_3} \leq f_{c_1}$ or f_{c_2} **then**
 - (25) remove c_3 ;
 - (26) **else**
 - (27) remove c_1, c_2 ;
 - (28) **end**
 - (29) **end**
 - (30) **next generation**
 - (31) **end**
 - (32) /* Ranking */ sort the F_p ;
 - (33) **return** $F_p[1]$ /* returns the most dominant solution w.r.t. fitness function */
- end**

ALGORITHM 3: Hyperparameter tuning of CNN using multiobjective genetic algorithm.

The genetic algorithm contains a group of operators to optimize the given fitness function [31]. Initially, random solutions are obtained using a normal distribution. These solutions are then applied to CNN for evaluating the multiobjective

fitness function (see equation (3)). Based on computed values, solutions are ranked for further processing. Thereafter, mutation and crossover operators are applied to the solutions for obtaining child values. Based upon their fitness values, they are

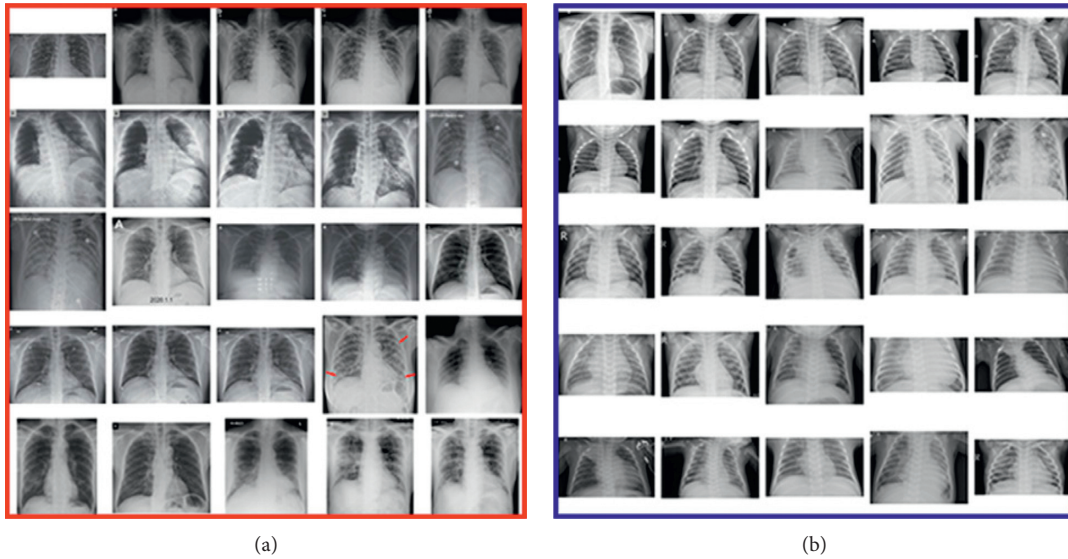


FIGURE 4: Chest X-ray image dataset: (a) normal persons' X-ray images, i.e., COVID-19 (-); (b) COVID-19-infected patients' X-ray images, i.e., COVID-19 (+).

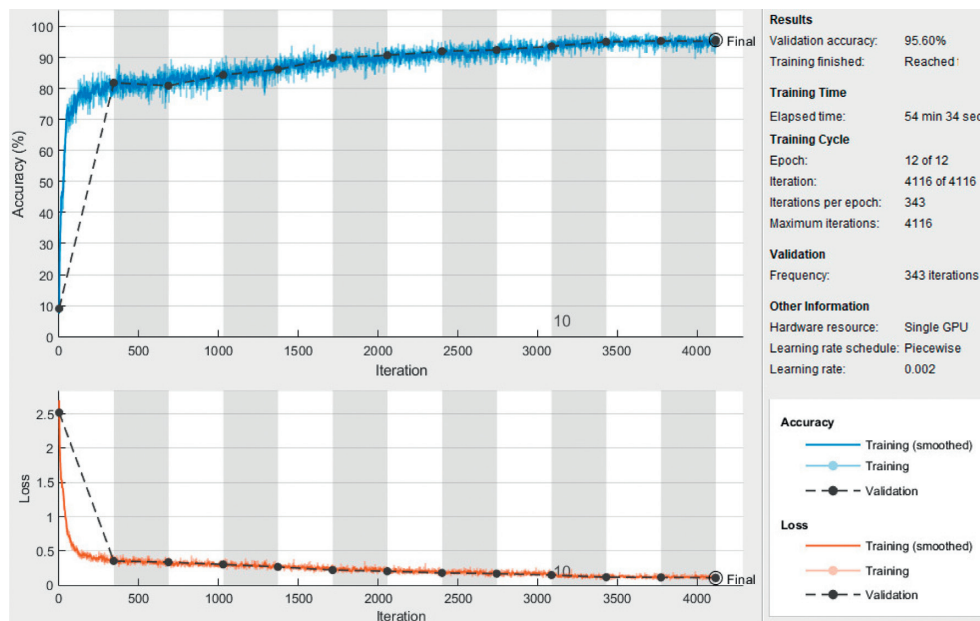


FIGURE 5: Training and validation analysis of the proposed COVID-19 identification model in terms of accuracy and loss.

ranked [32]. Finally, the most nondominated solution is returned as initial parameters of CNN.

4. Performance Analysis

This section discusses the performance analysis of the COVID-19 identification model. This work uses 20-fold cross-validation to overcome the overfitting problem. 70% of the entire dataset is considered for training purpose. The hyperparameters of the proposed COVID-19 identification model are obtained using a multiobjective genetic algorithm.

4.1. Chest X-Ray Image Dataset. To enhance prognostic analysis, triage and manage patient care, data is the first step for building any identification tool. Therefore, COVID-19 chest X-rays are collected to build COVID-19 identification models. Chest X-ray images of COVID-19-infected patients contain many unique characteristics. Therefore, chest X-ray images may be utilized to diagnose COVID-19-infected patients at a rapid speed.

In this paper, the chest X-ray images are obtained from several datasets such as from [2, 33]; there are 1332 COVID-19 (+) images and 1421 images of normal or pneumonia-infected patients. Figure 4 shows a partial set of X-ray images

TABLE 1: Training analysis of the COVID-19 identification models by utilizing confusion matrix-based performance metrics when training to testing ratio is 60 : 40.

Model	Accuracy	<i>F</i> -measure	Specificity	Sensitivity	AUC
SVM	0.872881	0.871186	0.871404	0.872666	0.872034
ANFIS	0.884746	0.883051	0.883249	0.868455	0.883898
CNN	0.894661	0.894915	0.895093	0.896435	0.895763
AlexNet	0.908475	0.906678	0.906937	0.908319	0.907627
ResNet-34	0.920339	0.918644	0.918782	0.920204	0.919492
GoogLeNet	0.932203	0.930508	0.930626	0.932088	0.931356
VGG-16	0.944068	0.942373	0.942747	0.943973	0.947322
ResNet-50	0.955932	0.954237	0.954315	0.955857	0.955085
Xception	0.967797	0.966102	0.966159	0.967742	0.966949
DenseNet201	0.979661	0.977966	0.978003	0.979626	0.978814
Proposed model	0.991525	0.989831	0.989848	0.991511	0.990678

TABLE 2: Testing (i.e., validation) analysis of the COVID-19 identification models by utilizing confusion matrix-based performance metrics when training to testing ratio is 60 : 40.

Model	Accuracy	<i>F</i> -measure	Sensitivity	Specificity	AUC
SVM	0.857627	0.864407	0.863481	0.858586	0.861017
ANFIS	0.869492	0.876271	0.875427	0.870537	0.872881
CNN	0.881356	0.888136	0.887372	0.882155	0.884746
AlexNet	0.893522	0.932324	0.899317	0.893939	0.895661
ResNet-34	0.905085	0.911864	0.911263	0.905724	0.908475
GoogLeNet	0.916949	0.923729	0.923208	0.917508	0.920339
VGG-16	0.928814	0.935593	0.935154	0.929293	0.932203
ResNet-50	0.940678	0.947458	0.947099	0.941077	0.944068
Xception	0.952542	0.959322	0.959044	0.952862	0.955932
DenseNet201	0.964407	0.971186	0.970949	0.964646	0.967797
Proposed model	0.976271	0.983051	0.982935	0.976431	0.979661

of normal persons and COVID-19-infected patients. It clearly shows that there is a significant change in the X-ray images of normal and COVID-19-infected patients.

4.2. Comparative Analysis. The performance of the proposed model is compared to various machine learning and deep learning approaches. The overall objective is to evaluate the significant improvement of the proposed model against various performance metrics such as accuracy, Area Under the Curve (AUC), *F*-measure, specificity, and sensitivity.

The training and validation analysis of the proposed COVID-19 identification model is illustrated in Figure 5. It demonstrates that the proposed COVID-19 identification model achieves significant training and validation accuracy values. It also indicates that the loss of the proposed COVID-19 identification model is minimum. Further, as the number of epoch increases, it shows improvement in results, but after 3300 epochs, it seems to be constant, i.e., not much improvement in results is observed.

Tables 1 and 2 show model building and testing analysis among the proposed and the existing COVID-19 identification models.

Table 1 reveals that the proposed model achieves significant performance in terms of accuracy, Area Under the

Curve (AUC), *F*-measure, specificity, and sensitivity as compared to the existing models.

5. Conclusion

In this paper, a CNN model is used to build COVID-19 identification model using the chest X-ray images. 20-fold cross-validation is used to overcome the overfitting problem. A pretrained GoogLeNet is also considered for implementing the transfer learning (i.e., by replacing some sets of final network CNN layers). Finally, the multiobjective genetic algorithm is used for hyperparameter tuning of the COVID-19 identification model. Performance analysis revealed that the COVID-19 identification model attains significantly good performance than the competitive models. The proposed COVID-19 identification model offered training and testing accuracy up to 98.3827% and 94.9383%, respectively. Thus, the designed identification model can be used for real-time identification of COVID-19 disease.

Data Availability

Data will be made available upon request.

Conflicts of Interest

The authors declare that they have no conflicts of interest.

References

- [1] E. E.-D. Hemdan, M. A. Shouman, and M. E. Karar, "Covidxnet: a framework of deep learning classifiers to diagnose COVID-19 in X-ray images," 2020, <http://arxiv.org/abs/2003.11055>.
- [2] D. Singh, V. Kumar, Vaishali, and M. Kaur, "Classification of COVID-19 patients from chest CT images using multi-objective differential evolution-based convolutional neural networks," *European Journal of Clinical Microbiology & Infectious Diseases*, vol. 39, no. 7, pp. 1379–1389, 2020.
- [3] S. Ayyachamy, V. Alex, M. Khened, and G. Krishnamurthi, "Medical image retrieval using Resnet-18," in *Medical Imaging 2019: Imaging Informatics for Healthcare, Research, and Applications*, vol. 10954, Bellingham, WA, USA, International Society for Optics and Photonics, Article ID 1095410, 2019.
- [4] Y. Pathak, K. V. Arya, and S. Tiwari, "An efficient low-dose ct reconstruction technique using partial derivatives based guided image filter," *Multimedia Tools and Applications*, vol. 78, no. 11, pp. 14733–14752, 2019.
- [5] Y. Yu, H. Lin, J. Meng, X. Wei, H. Guo, and Z. Zhao, "Deep transfer learning for modality classification of medical images," *Information*, vol. 8, no. 3, p. 91, 2017.
- [6] Y. Pathak, P. K. Shukla, A. Tiwari, S. Stalin, S. Singh, and P. K. Shukla, "Deep transfer learning based classification model for COVID-19 disease," *Biomedical Engineering and Research*, 2020, In press.
- [7] H. S. Pannu, D. Singh, and A. K. Malhi, "Improved particle swarm optimization based adaptive neuro-fuzzy inference system for benzene detection," *Clean—Soil, Air, Water*, vol. 46, no. 5, Article ID 1700162, 2018.
- [8] P. Tang, H. Wang, and S. Kwong, "G-MS2F: GoogLeNet based multi-stage feature fusion of deep CNN for scene recognition," *Neurocomputing*, vol. 225, pp. 188–197, 2017.
- [9] F. Gao, T. Wu, J. Li et al., "SD-CNN: a shallow-deep CNN for improved breast cancer diagnosis," *Computerized Medical Imaging and Graphics*, vol. 70, pp. 53–62, 2018.
- [10] S. Deepak and P. M. Ameer, "Brain tumor classification using deep CNN features via transfer learning," *Computers in Biology and Medicine*, vol. 111, Article ID 103345, 2019.
- [11] A. Çinar and M. Yildirim, "Detection of tumors on brain MRI images using the hybrid convolutional neural network architecture," *Medical Hypotheses*, vol. 139, Article ID 109684, 2020.
- [12] D. R. Nayak, R. Dash, and B. Majhi, "Automated diagnosis of multi-class brain abnormalities using MRI images: a deep convolutional neural network based method," *Pattern Recognition Letters*, vol. 138, 2020.
- [13] B. Liu, Q. Liu, Z. Zhu, T. Zhang, and Y. Yang, "MSST-Resnet: deep multi-scale spatiotemporal features for robust visual object tracking," *Knowledge-Based Systems*, vol. 164, pp. 235–252, 2019.
- [14] W. Hao, R. Bie, J. Guo, X. Meng, and S. Wang, "Optimized CNN based image recognition through target region selection," *Optik*, vol. 156, pp. 772–777, 2018.
- [15] S. Taheri and Ö. Toygar, "On the use of dag-CNN architecture for age estimation with multi-stage features fusion," *Neurocomputing*, vol. 329, pp. 300–310, 2019.
- [16] G. Ciocca, P. Napoletano, and R. Schettini, "CNN-based features for retrieval and classification of food images," *Computer Vision and Image Understanding*, vol. 176–177, pp. 70–77, 2018.
- [17] X. Liu, Y. Zhou, J. Zhao et al., "Multiobjective ResNet pruning by means of EMOAs for remote sensing scene classification," *Neurocomputing*, vol. 381, pp. 298–305, 2020.
- [18] C. Han and L. Shi, "ML-ResNet: a novel network to detect and locate myocardial infarction using 12 leads ECG," *Computer Methods and Programs in Biomedicine*, vol. 185, Article ID 105138, 2020.
- [19] M. Talo, O. Yildirim, U. B. Baloglu, G. Aydin, and U. R. Acharya, "Convolutional neural networks for multi-class brain disease detection using MRI images," *Computerized Medical Imaging and Graphics*, vol. 78, Article ID 101673, 2019.
- [20] N. N. Das, N. Kumar, M. Kaur, V. Kumar, and D. Singh, "Automated deep transfer learning-based approach for detection of COVID-19 infection in chest X-rays," *Biomedical Engineering and Research*, 2020, In press.
- [21] S. Liu, G. Tian, and Y. Xu, "A novel scene classification model combining ResNet based transfer learning and data augmentation with a filter," *Neurocomputing*, vol. 338, pp. 191–206, 2019.
- [22] M. Togacar, B. Ergen, and Z. Cömert, "COVID-19 detection using deep learning models to exploit social mimic optimization and structured chest X-ray images using fuzzy color and stacking approaches," *Computers in Biology and Medicine*, vol. 121, Article ID 103805, 2020.
- [23] H. S. Pannu, D. Singh, and A. K. Malhi, "Multi-objective particle swarm optimization-based adaptive neuro-fuzzy inference system for benzene monitoring," *Neural Computing and Applications*, vol. 31, no. 7, pp. 2195–2205, 2019.
- [24] S. Saha, K. M. Khabir, S. S. Abir, and A. Islam, "A newly proposed object detection method using faster R-CNN inception with ResNet based on Tensorflow," in *Real-Time Image Processing and Deep Learning 2019*, vol. 10996, International Society for Optics and Photonics, Bellingham, WA, USA, Article ID 109960X, 2019.
- [25] T. Wiens, "Engine speed reduction for hydraulic machinery using predictive algorithms," *International Journal of Hydromechatronics*, vol. 2, no. 1, pp. 16–31, 2019.
- [26] R. Wang, H. Yu, G. Wang, G. Zhang, and W. Wang, "Study on the dynamic and static characteristics of gas static thrust bearing with micro-hole restrictors," *International Journal of Hydromechatronics*, vol. 2, no. 3, pp. 189–202, 2019.
- [27] S. Osterland and J. Weber, "Analytical analysis of single-stage pressure relief valves," *International Journal of Hydromechatronics*, vol. 2, no. 1, pp. 32–53, 2019.
- [28] C. Cao, Y. Huang, Z. Wang, L. Wang, N. Xu, and T. Tan, "Lateral inhibition-inspired convolutional neural network for visual attention and saliency detection," in *Proceedings of the Thirty-Second AAAI Conference on Artificial Intelligence*, New Orleans, LA, USA, February 2018.
- [29] G. Qi, H. Wang, M. Haner, C. Weng, S. Chen, and Z. Zhu, "Convolutional neural network based detection and judgement of environmental obstacle in vehicle operation," *CAAI Transactions on Intelligence Technology*, vol. 4, no. 2, pp. 80–91, 2019.
- [30] C. Zhu, W. Yan, X. Cai, S. Liu, T. H. Li, and G. Li, "Neural saliency algorithm guide bi-directional visual perception style transfer," *CAAI Transactions on Intelligence Technology*, vol. 5, no. 1, pp. 1–8, 2020.
- [31] V. Roostapour, A. Neumann, and F. Neumann, "Evolutionary multi-objective optimization for the dynamic knapsack problem," 2020, <http://arxiv.org/abs/2004.12574>.

- [32] X. Xue, J. Lu, and J. Chen, "Using NSGA-III for optimising biomedical ontology alignment," *CAAI Transactions on Intelligence Technology*, vol. 4, no. 3, pp. 135–141, 2019.
- [33] J. P. Cohen, P. Morrison, and L. Dao, "COVID-19 Image Data Collection," 2020, <http://arxiv.org/abs/2003.11597>.